# Amplified total internal reflection

**J. Fan, A. Dogariu, L. J. Wang**

*NEC Laboratories America, 4 Independence Way, Princeton, NJ 08540 USA*
*Jfan@research.nj.nec.com*

**Abstract:** Totally internal reflected beams can be amplified if the lower-index medium has gain. We analyze the reflection and refraction of light, and analytically derive the expression for the Goos-Hänchen shifts of a Gaussian beam incident on a lower-index medium, both active and absorptive. We examine the energy flow and the Goos-Hänchen shifts for various cases. The analytical results are consistent with the numerical results. For the TE mode, the Goos-Hänchen shift for the transmitted beam is exactly half of that of the reflected beam, resulting in a "1/2" rule.



**OCIS codes:** (260.6970) Total internal reflection; (240.6690) Surface waves

## References and links

1. F. Goos and H. Hänchen, "Ein neuer und fundamentaler versuch zur totalreflexion," Ann. Phys. **1**, 23 (1947).
2. Von Kurt Artmann, "Berechnung der Seitenversetzung des totalreflektierten strahles," Ann. Phys. **1**, 87 (1948).
3. Helmut K. V. Lotsch, "Beam displacement at total reflection: the Goos Hänchen shift," OPTIK **32**, 116 (1970).
4. M. McGuirk and C. K. Carniglia, "An angular spectrum representation approach to the Goos Hänchen shift," J. Opt. Soc. Am. **67**, 103 (1976).
5. F. Bretenaker, A. L. Floch, and L. Dutriaux, "Direct measurement of the optical Goos-Hänchen effect in lasers," Phys. Rev. Lett. **17**, 931 (1992).
6. S. Kozaki and H. Sakurai, "Characteristics of a Gaussian beam at a dielectric interface," J. Opt. Soc. Am. **68**, 508 (1978).
7. C. J. Koester, "9A4-Laser action by enhanced total internal reflection," IEEE J. Quantum Electron. **QE-2**, 580 (1966).
8. E. P. Ippen and C. V. Shank, "Evanescent-field-pumped dye laser," Appl. Phys. Lett. **21**, 301 (1972).
9. K. O. Hill, A. Watanabe, and J. G. Chambers, "Evanescent-wave interactions in an optical wave-guiding structures," Appl. Opt. **11**, 1952 (1972).
10. W. Y. Liu and O. M. Stafsudd, "Optical amplification of a multimode evanescently active planar optical waveguide," Appl. Opt. **29**, 3114 (1990).
11. E. Pfleghaar, A. Marseille, and A. Weis, "Quantative investigation of the effect of resonant absorpers on the Goos-Hänchen shift," Phys. Rev. Lett. **12**, 2281 (1993).
12. B. Ya. Kogan, V. M. Volkov, and S. A. Lebedev, "Superluminescence and generation of stimulated radiation under internal-reflection conditions," JETP Lett. **16**, 100 (1972).
13. G. N. Romanov and S. S. Shakhidzhanov, "Amplification of electromagnetic field in total internal reflection from a regeion of inverted population," JETP Lett. **16**, 209 (1972).
14. S. A. Lebedev, V. M. Volkov, and B. Ya. Kogan, "Value of the gain for light internally reflected from a medium with inverted population," Opt. Spectrosc. **35**, 565 (1973).
15. P. R. Callary and C. K. Carniglia, "Internal reflection from an amplifying layer," J. Opt. Soc. Am. **66**, 775 (1976).
16. W. Lukosz and P. P. Herrmann, "Amplification by reflection from an active medium," Optics Comm. **17**, 192 (1976).
17. R. F. Cybulski, Jr. and C. K. Carniglia, "Internal reflection from an exponential amplifying region," J. Opt. Soc. Am. **67**, 1620 (1977).
18. S. A. Lebedev and B. Ya. Kogan, "Light amplification by internal reflection from an inverted medium," Opt. Spectrosc. **48**, 564 (1980).

#1930 - $15.00 US Received December 12 2002; Revised February 12, 2003

19. R. F. Cybulski and M. P. Silverman, "Investigation of light amplification by enhanced internal reflection. I. Theoretical reflectance and transmittance of an exponentially nonuniform gain region," J. Opt. Soc. Am. **73**, 1732 (1983).
20. M. P. Silverman and R. F. Cybulski, "Investigation of light amplification by enhanced internal reflection. II. Experimental determination of the single-pass reflectance of an optically pumped gain region," J. Opt. Soc. Am. **73**, 1739 (1983).
21. Max Born and Emil Wolf, *Principles of Optics*, 6th edition (Cambridge, 1997).
22. J. W. Goodman, *Introduction to fourier optics* (McGraw-Hill, 1968), Chap. 3.

## 1. Introduction

Reflection of light at the surface between two different media has always been an interesting topic. Total internal reflection occurs when a light beam is incident from a medium of higher refractive index onto a medium of lower refractive index, at greater than or equal to the critical angle. The incident beam is completely reflected, with no attenuation. The reflected beam, however, is laterally displaced from the position predicted by geometrical optics, this is known as the Goos-Hänchen shift [1-6]. The reflection of a beam on a lower-index medium with gain (inverted or active) or loss (absorptive) is especially interesting, not only because of the abundant physics but also because of its wide applications [7-20]. The reflection of a beam on a lower-index absorptive medium at greater than the critical angle is known as the attenuated total internal reflection (ATIR), where the reflectivity is less than unity, and the transmitted beam propagates inhomogeneously with attenuation [21]. In the case of a beam incident on a lower-index active medium at beyond the critical angle, there has been a concern of the propagation and gain about the transmitted and reflected beams [12-20].

In this paper, we investigate the reflection and refraction of a Gaussian beam by a lower-index medium, either active (any isotropic optically active gain medium, such as optically pumped dye solutions or inverted atomic systems, etc.) or absorptive (any isotropic loss medium). We numerically examine the energy flux and the Goos-Hänchen shift. The paper is organized as following. In Section 2, we discuss the reflection of a plane wave on a planar interface between two different media. In Section 3, considering the reflection of a Gaussian beam at a planar interface between two different media, we analytically derive the expression of Goos-Hänchen shift in a more general sense, and analyze the properties of Goos-Hänchen shift for a pair of conjugate loss and gain media (explained below). In section IV, a numerical calculation is carried out, and a comparison is made with the analytical results obtained in Section 3. We summarize our findings in Section 5

## 2. Reflection of a plane wave at an interface between two different media

First, we consider the reflection of a plane wave at a planar interface between two different isotropic media. The geometry and coordinates are shown in Fig. 1(a). A two dimensional picture is used, and the electromagnetic field is assumed to have no y-dependence. The two semi-infinite space separated by a planar interface are filled with media of different relative permittivities, $\varepsilon_1$ and $\varepsilon_2 = (\varepsilon_R + i\varepsilon_I)$, respectively. $\varepsilon_1 > \varepsilon_R$ and $\varepsilon_I$ are real. $\theta$ is the incident angle. The critical angle is defined as $\theta_c = \sin^{-1}\sqrt{\varepsilon_R / \varepsilon_1}$. For simplicity, the relative permeabilities are assumed to be unity. The reflective and refractive coefficients are, as given by the Fresnel's law,

$$r(k_{ix}, \varepsilon_1, \varepsilon_2) = \frac{\eta k_{iz} - k_{tz}}{\eta k_{iz} + k_{tz}} \tag{1a}$$

$$t(k_{ix}, \varepsilon_1, \varepsilon_2) = \frac{2\eta k_{iz}}{\eta k_{iz} + k_{tz}} \quad , \tag{1b}$$

#1930 - $15.00 US Received December 12 2002; Revised February 12, 2003

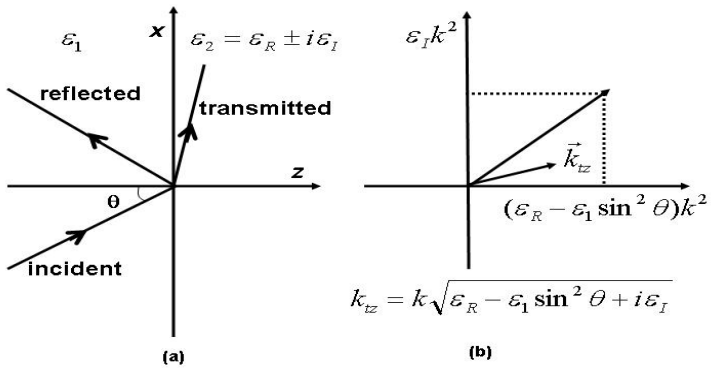


Fig. 1. (a) The geometry and coordinate system of the reflection of a plane wave on a planar interface between two different media; (b) illustration of $k_{tz}$ as a root solution in a complex coordinate plane.

respectively [21]. Here $\eta = 1$ for the TE mode and $\sqrt{\varepsilon_2 / \varepsilon_1}$ for the TM mode; $k_{ix} = \sqrt{\varepsilon_1} k \sin\theta$ and $k_{iz} = \sqrt{\varepsilon_1} k \cos\theta$ are the propagation wave numbers along the *x*- and the *z*- axes in the higher-index medium. $k$ is the vacuum wave number; $k_{tz} = \pm k\sqrt{\varepsilon_R - \varepsilon_1 \sin^2\theta + i\varepsilon_I} = k_R + i\kappa$ is the complex wave number along *z*-axis in the lower-index medium as shown in Fig. 1(b). The choice of sign for $k_{tz}$ is discussed in the following. The real propagation wave number $k_R$, and the coefficient $\kappa$ representing the gain or loss, depend on the medium, and satisfy the following equations,

$$k_{ix}^2 + k_R^2 - \kappa^2 = \varepsilon_R k^2, \tag{2a}$$

$$2k_R\kappa = \varepsilon_I k^2. \tag{2b}$$

Obviously, Eq. (2b) requires that $k_R$ and $\kappa$ are of the same sign if $\varepsilon_I > 0$, and opposite sign if $\varepsilon_I < 0$.

(*a*) *Below the critical angle*, $k_{tz}^2$ is in the first or the fourth quadrant in Fig. 1(b), for $\varepsilon_I > 0$ and $\varepsilon_I < 0$, respectively. The dashed lines in Fig. (2a) and (2b) show $k_R$ versus $\varepsilon_I$, and $\kappa$ versus $\varepsilon_I$, at less than $\theta_c$. For a pair of conjugate loss and gain media, i.e. with $\varepsilon_2$ and $\varepsilon_2^*$, respectively, according to Eq. (1a) and (1b), the reflective and refractive coefficients are conjugate:

$$r^*(k_{ix}, \varepsilon_1, \varepsilon_2) = r(k_{ix}, \varepsilon_1, \varepsilon_2^*) \tag{3a}$$

$$t^*(k_{ix}, \varepsilon_1, \varepsilon_2) = t(k_{ix}, \varepsilon_1, \varepsilon_2^*) \tag{3b}$$

Therefore, the energy flux across the interface for a plane wave incident on an active medium is the same as that of a plane wave incident on a conjugate absorptive media. This manifests on the symmetrical behavior of both the reflectivity and transmissivity for conjugate media, as is shown in Fig. 2(d), where we plot the z-component of the Poynting vector given by $S_{z,reflected} = -|r|^2$ and $S_{z,transmitted} = |t|^2 k_R / k_{iz}$, respectivelly. As indicated by the dashed curve in Fig. 2(a), for any $\varepsilon_I$, we always have $k_R > 0$. There is a real propagating electromagnetic field with a wave number $k_R$ for media with either gain or loss.

#1930 - $15.00 US Received December 12 2002; Revised February 12, 2003

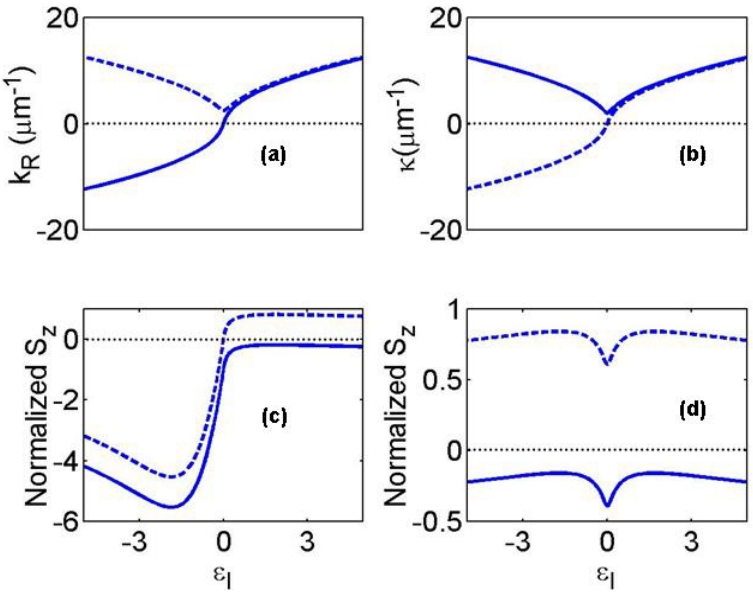


Fig. 2. $k_{tz}$ and energy flux across the interface vs $\varepsilon_I$ for TE mode, $\varepsilon_1$=3.24, $\varepsilon_2$=1.44±i$\varepsilon_I$, , $\theta_c$=41.8°. (a) $k_R$ vs. $\varepsilon_I$ , smooth line: $\theta$=43°>$\theta_c$, dashed line: $\theta$=40°<$\theta_c$; (b) $\kappa$ vs. $\varepsilon_I$, smooth line: $\theta$=43°, dashed line: $\theta$=40°; (c)z-component Poynting vectors of the reflected and transmitted beam normalized to that of the incident beam, $\theta$=43°. Smooth line: reflected beam, dashed line: transmitted beam; (d) same as in (c), $\theta$=40°. Quantities are evaluated at the interface.

(b) *Beyond the critical angle*, if $\varepsilon_I>0$, $k_{tz}^2$ is in the second quadrant in Fig. 1(b), and attenuated total internal reflection occurs. The reflectivity perpendicular to the interface, calculated as the z-component of the Poynting vector, is always less than unity as shown in Fig. 2(c). When a beam is incident on an active medium ($\varepsilon_I<0$) at beyond the critical angle, $k_{tz}^2$ is in the third quadrant of Fig. 1(b). It was thought that $k_{tz}$ for the transmitted beam could be either in the second or the fourth quadrant [12-20]. If $k_{tz}$ is in the fourth quadrant (more exactly, between 270° and 315° in the $k_R$-$\kappa$ complex plane), the excited electromagnetic field in the lower-index medium would propagate along *z*-axis with gain. When $\varepsilon_I$ is very small, (the lower-index medium basically has no population inversion), the "gain" is of order $e^{zk\sqrt{\varepsilon_1 \sin^2\theta-\varepsilon_R}}$, which can be any large number. So, although a possible mathematical solution, the fourth quadrant $k_{tz}$ is not an appropriate physical solution. On the other hand, if $k_{tz}$ is in the second quadrant (more exactly, between 90° and 135° in the $k_R$-$\kappa$ complex plane), in the limit of $\varepsilon_I \to 0$, the situation returns to the total internal reflection, an evanescent field is excited in the lower-index medium to the depth of ~1/$\kappa_0$, where $\kappa_0 = k\sqrt{\varepsilon_1 \sin^2\theta-\varepsilon_R}$. This only possible solution of using the second quadrant $k_{tz}$ reveals a very interesting physical picture. Here, the electromagnetic field is excited in the lower-index medium within the depth of ~$1/\kappa$; and propagates backwards toward the interface with gain $e^{-\kappa z}$, where $k_R$ and $\kappa$ are given as:

$$k_R = -\frac{k}{\sqrt{2}}\left[\sqrt{(\varepsilon_R-\varepsilon_1\sin^2\theta)^2+\varepsilon_I^2}+(\varepsilon_R-\varepsilon_1\sin^2\theta)\right]^{1/2}, \quad (4a)$$

and

$$\kappa = \frac{k}{\sqrt{2}}\left[\sqrt{(\varepsilon_R-\varepsilon_1\sin^2\theta)^2+\varepsilon_I^2}-(\varepsilon_R-\varepsilon_1\sin^2\theta)\right]^{1/2}. \quad (4b)$$

#1930 - $15.00 US Received December 12 2002; Revised February 12, 2003

Therefore, the reflected beam is more intense compared to the incident beam, this is the enhanced total internal reflection effect (ETIR). The gain of the reflected beam is limited as shown in Fig. 2(c) (smooth line). We note the non-monotonic behavior of the amplification.
As indicated by the smooth curve in Fig. 2(a), for $\varepsilon_I \neq 0$, there is a real propagating electromagnetic field with a wave number $k_R$ for media with either gain or loss. For $\varepsilon_I = 0$, we have $k_R = 0$, only evanescent field exists in the lower-index medium.

### 3. Reflection of a Gaussian beam on an active or absorptive medium

The total reflection of a Gaussian beam has been well treated in the literature. The Goos-Hänchen shift was generally obtained by taking the first order derivative of the phase of the electromagnetic field with respect to the wave number [1-6]. Here, we generalize this approach and derive the expression of the Goos-Hänchen shift when a Gaussian beam is incident on an active or absorptive medium. A monochromatic Gaussian beam is assumed in the discussion for simplicity, and a two-dimensional picture is also used.

Let us consider a monochromatic Gaussian beam as the collection of different propagation modes, $e^{i\vec{k}\cdot\vec{r}}$, which can be characterized by the transverse wave number $k_{ix}$ [22]. In total internal reflection, each individual mode has a different phase shift at the interface. This results in the redistribution of the electromagnetic field for the reflected and the transmitted beams via interference. It has been well-known and generally applied that, given the electromagnetic field in the representation of time-space, from time-frequency and space-momentum duality, the instant frequency at $t=t_0$ and wave vector at $\vec{r} = \vec{r}_0$ can be obtained as the phase variation with respect to the time and space, $\omega = (\frac{\partial \phi(t,\vec{r})}{\partial t})_{t=t_0}$ and $\vec{k} = (\frac{\partial \phi(t,\vec{r})}{\partial \vec{r}})_{\vec{r}=\vec{r}_0}$, respectively. Similarly, given the electromagnetic field in the representation of energy-momentum, we have

$$x = (\frac{\partial \phi(\omega,\vec{k})}{\partial k_x})_{k_x=k_{x0}}. \tag{5}$$

We consider a well-collimated monochromatic Gaussian beam, with all significant wave vector components incident at either beyond or below the critical angle. Each individual propagation mode of the reflected and the transmitted beam can be treated as a plane wave and hence receives a phase shift at the interface given by

$$\phi_r(k_{ix}) = \mathrm{Im}[\ln(r)] \tag{6a}$$

$$\phi_t(k_{ix}) = \mathrm{Im}[\ln(t)], \tag{6b}$$

where $r$ and $t$ are the reflective and refractive coefficients for the TE or TM modes given in Eq. (1a) and (1b). According to Eq. (5), and assuming the same plane-wave expressions for all $k_{ix}$, $k_{iz}$, and $k_{tz}$ given in Section 2, which proves to be a very good approximation in the later numerical calculation, we have

$$\bar{x}_r = \frac{\partial \phi(k_{ix})}{\partial k_{ix}} = 2\tan\theta\,\mathrm{Im}\left(\frac{1}{k_{tz}}\frac{\eta(k_{iz}^2 - k_{tz}^2)}{(\eta^2 k_{iz}^2 - k_{tz}^2)}\right) \tag{7a}$$

$$\bar{x}_t = \tan\theta\,\mathrm{Im}\left(\frac{1}{k_{iz}k_{tz}}\frac{k_{iz}^2 - k_{tz}^2}{\eta k_{iz} + k_{tz}}\right), \tag{7b}$$

where $\bar{x}_r$ and $\bar{x}_t$ are the Goos-Hänchen shifts for the reflected and transmitted beam, respectively, and $\eta$ is given in Eq. (1). It is easy to prove that, below the critical angle, the shifts are anti-symmetrical, $\bar{x}_r(\varepsilon_2) = -\bar{x}_r(\varepsilon_2^*)$ and $\bar{x}_t(\varepsilon_2) = -\bar{x}_t(\varepsilon_2^*)$, for conjugate permittivities.

#1930 - $15.00 US Received December 12 2002; Revised February 12, 2003

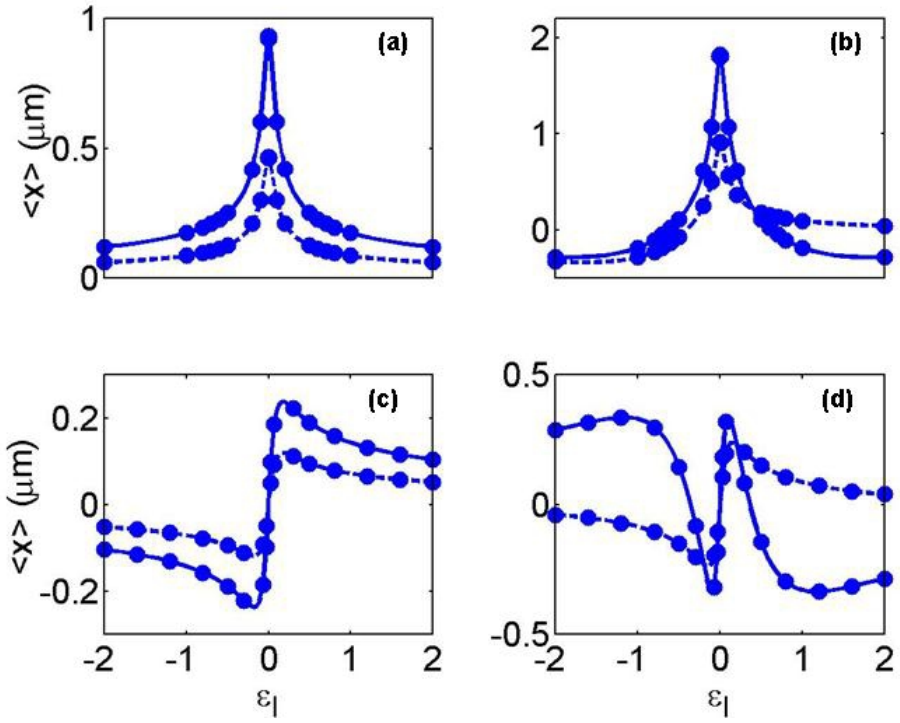


Fig. 3. Goos Hänchen shifts vs $\varepsilon_I$. Smooth lines and dashed lines are shifts for the reflected and transmitted beams, respectively, obtained using Eq. (7). Dotted lines are from the numerical calculation using angular spectrum method [22]. $\varepsilon_1$=3.24, $\varepsilon_2$=1.44±i$\varepsilon_I$, $\theta_c$=41.8°. (a) and (c) are for the TE mode, (b) and (d) are for the TM mode. Incident angle is $\theta$=43° in (a) and (b), $\theta$=40° in (c) and (d).

For the TE mode, $\eta$=1, we have, from Eq. (7a) and (7b),

$$\bar{x}_r = 2\tan\theta\,\mathrm{Im}\left(\frac{1}{k_{tz}}\right), \tag{8a}$$

and

$$\bar{x}_t = \tan\theta\,\mathrm{Im}\left(\frac{1}{k_{tz}} - \frac{1}{k_{iz}}\right). \tag{8b}$$

Because the incident wave number $k_{iz}$ is real, this results in a "1/2" rule,

$$\bar{x}_t = \frac{1}{2}\bar{x}_r = \tan\theta\,\mathrm{Im}\left(\frac{1}{k_{tz}}\right) = -\tan\theta\frac{\kappa}{|k_{tz}^2|}\quad . \tag{9}$$

This relation obviously holds for both incidences at beyond or below the critical angle. Equation (9) shows that the Goos-Hänchen shifts and $\kappa$ have the same symmetry and anti-symmetry pattern for conjugate media. Specifically, beyond the critical angle, the Goos-Hänchen shifts are symmetrical for conjugate media, and peak at the total internal reflection condition $\varepsilon_I = 0$, as shown by the lines in Fig. 3(a). Less than the critical angle, the Goos-Hänchen shifts are anti-symmetrical for conjugate media, and vary smoothly through zero when $\varepsilon_I$ changes sign, as shown by the lines in Fig. 3(c). The Goos-Hänchen shifts can be of the order of a wavelength when the beam is incident at close to the critical angle.

#1930 - $15.00 US
Received December 12 2002; Revised February 12, 2003

Beyond the critical angle and for an active medium, if the fourth quadrant $k_{tz}$ would be used, the Goos-Hänchen shifts would have the same amount, but in opposite directions, as opposed to the above case of using the second quadrant for $k_{tz}$. So, besides the physical consideration discussed in Section 2, experimentally examining the Goos-Hänchen shift can verify the validity of Eq. (4).

For the TM mode, beyond the critical angle, the Goos-Hänchen shift is also symmetrical for the reflected beam, as shown by the smooth line, and generally asymmetrical for the transmitted beam, as shown by the dashed line in Fig. 3(b). The shifts peak at $\varepsilon_1 = 0$, and decrease and even become negative with increasing $|\varepsilon_1|$. Below the critical angle, when $\varepsilon_1$ changes from negative to positive, the shift of the reflected beam changes dramatically, as shown in Fig. 3(d). The peak shifts can be on the order of the wavelength when the incidence angle is close to $\theta_c$.

**4. Numerical calculation**

In the above discussion, the Goos-Hänchen shifts are obtained as the first order phase variation with respect to the transverse wave number $k_{ix}$. Because of the phase discontinuity at the critical angle, the higher order propagation modes and the case of beam incident at close or equal to the critical angle cannot be treated analytically. In this section, using the angular spectrum method [22], we numerically investigate the reflection of a Gaussian beam on an active or absorptive medium without approximation, and compare these results with the analytical results obtained in Section 3.

The laboratory coordinate system is the same as in Fig. 1(a), where the incidence plane lies in the x-z plane, and the Gaussian beam arrangement is the same as in the Ref. [6]. Using the angular spectrum method, for the TE mode, the propagation of the Gaussian beam, in its own coordinates, is expressed as [22]

$$E(x_1, z_1) = \int_{-\infty}^{+\infty} dk_{1x} E(k_{1x}, z_0) e^{i(k_{1x}x_1 + k_{1z}z_1)}, \tag{10}$$

where $E(k_{1x}, z_0) = \frac{aE_0}{\sqrt{2\pi}} e^{-(\frac{k_{1x}}{\sqrt{2}/a})^2}$ is the electric field amplitude of the propagation mode $e^{i(k_{1x}x_1 + k_{1z}z_1)}$ at $z=z_0$ in the angular spectrum representation (or momentum space), and $a$ is the *1/e* radius of the Gaussian beam intensity profile. The $z_1$ axis is selected to be along the optical propagation axis of the Gaussian beam such that the transversal momentum averages to zero,

$$< k_{1x} >= \int_{-\infty}^{+\infty} E(k_{1x}) k_{1x} E^*(k_{1x}) dk_{1x} = 0 \tag{11}$$

In the laboratory coordinate system, the electric field of the incident Gaussian beam can be written as

$$E_i(x, z) = E(x_1, z_1) = \int_{-\infty}^{+\infty} dk_{1x} E(k_{1x}, z_0) e^{i(k_{1z}x + k_{1z}z_1)} = \int_{-\infty}^{+\infty} dk_{ix} f(k_{ix}) e^{i(k_{ix}x + k_{iz}z)}, \tag{12a}$$

where $f(k_{ix}) = (\cos\theta + \frac{k_{ix}\sin\theta}{\sqrt{\varepsilon_1 k^2 - k_{ix}^2}}) E(k_{1x}, z_0)$ is the electric field amplitude of the propagation mode $e^{i(k_{ix}x + k_{iz}z)}$, and $\theta$ is the incident angle of the Gaussian beam. The electric fields of the reflected and transmitted beams can be written as

$$E_r(x, z) = \int_{-\infty}^{+\infty} dk_{ix} r_{TE}(k_{ix}) f(k_{ix}) e^{i(k_{ix}x - k_{iz}z)} = \int_{-\infty}^{+\infty} dk_{1x} r_{TE}(k_{ix}) E(k_{1x}, z_0) e^{i(k_{ix}x - k_{iz}z)} \tag{12b}$$

$$E_t(x, z) = \int_{-\infty}^{+\infty} dk_{ix} t_{TE}(k_{ix}) f(k_{ix}) e^{i(k_{ix}x - k_{iz}z)} = \int_{-\infty}^{+\infty} dk_{1x} t_{TE}(k_{ix}) E(k_{1x}, z_0) e^{i(k_{ix}x + k_{iz}z)}, \tag{12c}$$

#1930 - $15.00 US Received December 12 2002; Revised February 12, 2003

where $r_{TE}(k_{ix})$ and $t_{TE}(k_{ix})$ are the reflective and refractive coefficients for each individual mode given in Eq. (1).

The magnetic field *H* of the beams can be obtained in the same way. For z<0, the total electromagnetic fields result from the interference of the incident and the reflected beams; for z>0, they are that of the transmitted beam. The time-averaged Poynting vector can be obtained using $\vec{S} = \frac{1}{2}\mathrm{Re}(\vec{E} \times \vec{H}^*)$.

The Goos-Hänchen shifts are expressed as the statistical average of the transversal position *x* at the interface,

$$< x >_p = \frac{< E_p(x,z) x E_p^*(x,z) >_x}{< E_p(x,z) E_p^*(x,z) >_x}, \tag{12}$$

where *p* can be *i, r,* and *t*. $E_p$ stands for the incident, reflected, or transmitted electric fields, respectively.

The incident Gaussian beam is assumed to be monochromatic with $\lambda = 800nm$ and $a=17\mu m$, and the peak amplitude is chosen to be *0.2V/m* for *E* in the TE mode, and *0.2A/m* for *H* in the TM mode in the calculation.

The calculated Goos-Hänchen shifts are shown as the dots in Fig. (3), which perfectly match the analytical results. The consistency between the numerical results and the analytical results shows that the analytical approach in deriving the Goos-Hänchen shifts and the analytical results are generally valid, when the incident angle is not too close to the critical angle.

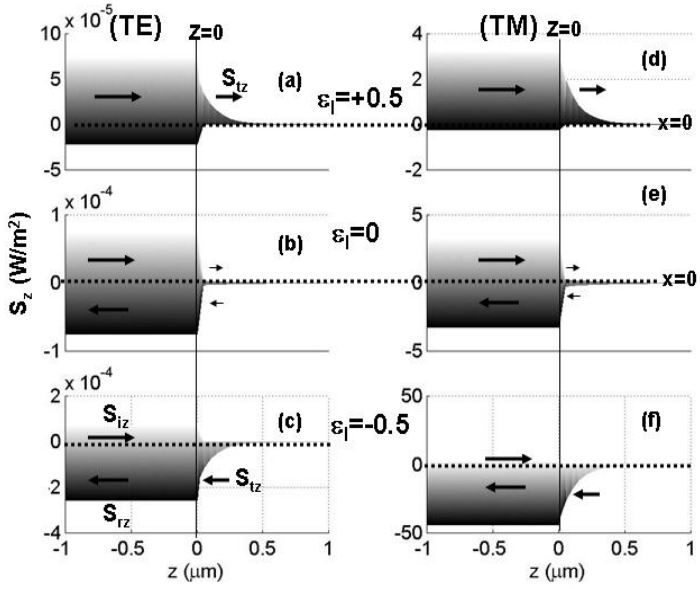


Fig. 4. Projection of z-component energy flux for the incident $S_{iz}$, reflected $S_{rz}$ and refracted beams $S_{tz}$ at x-z plane. $\varepsilon_1$=3.24, $\varepsilon_1$=1.44±$\varepsilon_I$, $\theta_c$=41.8°. Gaussian beam: *a=17μm*, with peak amplitude 0.2V/m for the electric field in the TE mode and 0.2A/m for the magnetic field in the TM modes. $S_z$ is along +z if positive, –z if negative, as shown by the arrows. Dotted line shows the center of the incident Gaussian beam.

Figure 4 shows the calculated energy flux of a Gaussian beam incident at beyond the critical angle. In the case of an absorptive medium, the transmitted beam attenuates after propagating a distance on the order of the wavelength, as shown in Fig. 4(a) and 4(d). At total internal reflection, the energy transfers from the incident beam into the lower-index medium,

then flows back to the higher-index medium, such that the reflectivity is unity, as shown in Fig. 4(b) and 4(e). In the case of an active medium, the gain length is again on the order of a wavelength in the lower-index medium. The electromagnetic field propagates with gain backwards toward the interface where it combines with the incident beam to result in an enhanced reflected beam, as shown in Fig. 4(c) and 4(f).

The electric fields corresponding to the energy flux of the TE modes are shown in Fig. 5(a-c). In the region z<0, the electric fields of the incident and reflected beams interfere to form a periodical pattern. The intensity appears weaker when ε>0 (ATIR) and stronger when ε<0 (ETIR). In the region z>0, the evanescent field of the total reflection is excited deeper than the propagation depth of the transmitted beams of ETIR and ATIR. The calculated beam centers are plot in Fig. 5(d-f) with the propagation direction labeled by the arrows, corresponding to the incident, reflected, and transmitted beams, respectively. At the interface, the reflected and transmitted beams shift from the positions predicted by geometrical optics, and these shifts follow the "1/2" rule. The difference between the transmitted beams in conjugate media results from the fact that the complex propagation modes $k_{tz}$ are in different quadrants, as discussed in section II. The propagation of the transmitted beam can still be described using the Snell's law. With the effective refractive index $n_{eff}$ and the effective angle $\theta_{eff}$, we have $n_{eff}\sin\theta_{eff} = \sqrt{\varepsilon_1}\sin\theta$, where $n_{eff} = \sqrt{\varepsilon_1 \sin^2\theta + (\mathrm{Re}\sqrt{\varepsilon_2 - \varepsilon_1 \sin^2\theta})^2}$.

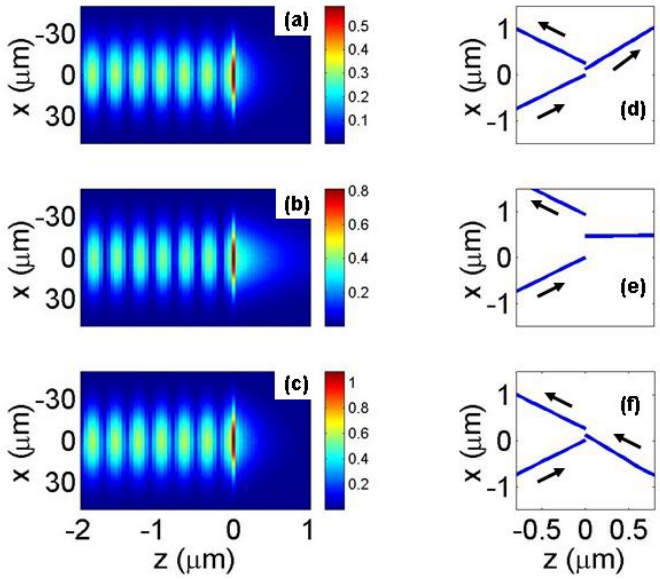


Fig. 5. Electric fields (a-c) and beam centers (d-f) for the TE mode. (a)(d), $\varepsilon_I$=+0.5; (b)(e), $\varepsilon_I$=0; (c)(f), $\varepsilon_I$=-0.5; other conditions are the same as in Fig. 4. The arrows in (d)-(f) show the propagation directions of different beams.

Figure 6 shows the calculated z-component energy flux of the transmitted beam at the interface. From top to bottom, the figures show that the energy transferred from the incident beam: (a) is completely absorbed in the lower-index medium when the medium is strongly absorptive ($\varepsilon_I$=+0.1) , (b) flows back to the higher-index medium with attenuation when the medium is weakly absorbing ($\varepsilon_I$=+0.01), (c) flows back to the higher-index medium without attenuation at total reflection ($\varepsilon_I$=0), (d) flows back to the higher-index medium with small gain when the medium is weakly inverted ($\varepsilon_I$=-0.01), and (e) propagates backwards toward the interface with significant gain when the medium is more active ($\varepsilon_I$=-0.1).

#1930 - $15.00 US Received December 12 2002; Revised February 12, 2003

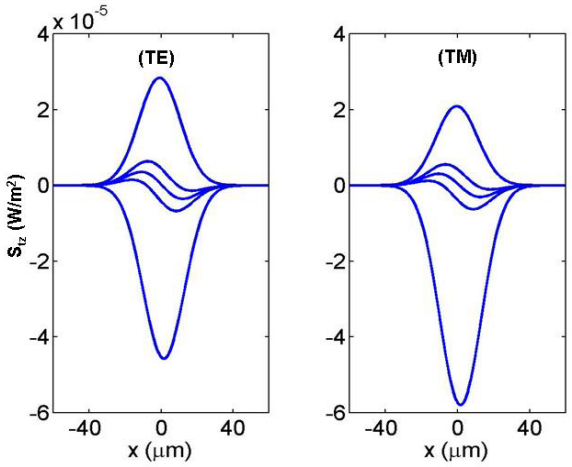


Fig. 6. Energy flux of the refracted beam $S_{tz}$, as a function of x at the interface. In each subplot, from top to bottom, curves correspond to $\varepsilon_1$=0.1, 0.01, 0, -0.01, -0.1, respectively. Other conditions are the same as in Fig. 4.

## 5. Summary

We have studied the reflection of a light beam incident from a medium with higher-index, onto a lower-index medium with gain or loss. We find that, beyond the critical angle, for a lower-index active medium, the transmitted beam propagates backwards toward the interface with gain.

We analytically obtain the expression for the Goos-Hänchen shift of a Gaussian beam incident on a lower-index medium. Less than the critical angle, the Goos-Hänchen shifts are anti-symmetrical for a pair of conjugate media. Beyond the critical angle, for the TE mode, the Goos-Hänchen shifts are symmetrical for conjugate media. Furthermore, the shift for the transmitted beam is half of that of the reflected beam. For the TM mode, for conjugate media, the Goos-Hänchen shift is symmetrical for the reflected beam, and generally asymmetrical for the transmitted beam.

Using angular spectrum method, without approximation, we numerically calculate the energy flow and the Goos-Hänchen shift for a Gaussian beam incident on a lower-index active or absorptive medium. The consistency between the numerical results and the analytical treatment shows that the analytical approach in deriving the Goos-Hänchen shifts is valid and very good, except for incidence angles very close to the critical angle.

The interesting situation of a light pulse incident onto a lower-index active or absorptive medium and various time-dependent field effects will be analyzed elsewhere. To further understand the physical process, an approach in the point of view of quantum theory is also needed and will be treated in future work.


## Acknowledgements

The authors wish to acknowledge the helpful discussions with A. E. Siegman.